PERGAMON

International Journal of Solids and Structures 38 (2001) 8831–8850

INTERNATIONAL JOURNAL OF SOLIDS and STRUCTURES

www.elsevier.com/locate/ijsolstr

The web bridge

Riccardo Barsotti [a], Salvatore S. Ligarò [a], Gianni F. Royer-Carfagni [b,*]

[a] *Department of Structural Engineering, University of Pisa, Via Diotisalvi 2, I-56126 Pisa, Italy*
[b] *Department of Civil Engineering, University of Parma, Parco Area delle Scienze 181/A, I-43100 Parma, Italy*

Received 21 June 2000; in revised form 2 May 2001

Abstract

Optimal cable arrangements for tensile structures, for bridges in particular, are determined by drawing inspiration from the wrinkling behavior of flat elastic membranes stretched in their plane. The underlying rationale for the approach consists in the fact that wrinkle patterns naturally develop according to a "maximum-stiffness" criterion. By way of illustration, a two-dimensional theory is proposed to model the wrinkling phenomenon in membranes subjected to general in plane loading, and an iterative procedure is then presented for solving numerically the governing set of non-linear equilibrium equations in a finite-element framework. The numerical results show good agreement with experiments performed on thin polyethylene sheets. An idealized web bridge is then conceived of, in which the deck is regarded as being sustained by an elastic membrane. A simple criterion is then used to pass from the continuous natural wrinkled equilibrium configuration of the membrane to a discrete layout, formed by a cable net, exploitable in the design of a real bridge. By changing the parameters controlling the shape of the web, various "optimal" cable arrangements are determined. These turn out to resemble classical cable-stayed bridges or mixed suspended and cable-stayed "hybrid" solutions.

Keywords: Shape optimization; Tensile structures; Wrinkled membranes; Cable-stayed bridges; Suspension bridges

1. Introduction

Despite the importance of determining optimal structural shapes for bridges, just formulating the problem presents formidable difficulties, because optimal solutions must simultaneously account for economy, serviceability and (why not?) aesthetics as well. The underlying idea of this work consists of seeking to determine optimal cable arrangements for typical tensile structures, such as cable-stayed or suspension bridges, by drawing inspiration from the natural response of flat elastic membranes stretched in their plane.

The approach stems from observations of the particular behavior of membranes. Because of their well-known inability to locally sustain or transmit any bending or twisting couples, membranes show a characteristic extensional response: whereas considerable stiffness is displayed under tension, when the sign of

* Corresponding author. Tel.: +39-521-905923; fax: +39-521-905924.
E-mail address: royer@dic.eng.unipr.it (G.F. Royer-Carfagni).

0020-7683/01/$ - see front matter
PII: S0020-7683(01)00115-9

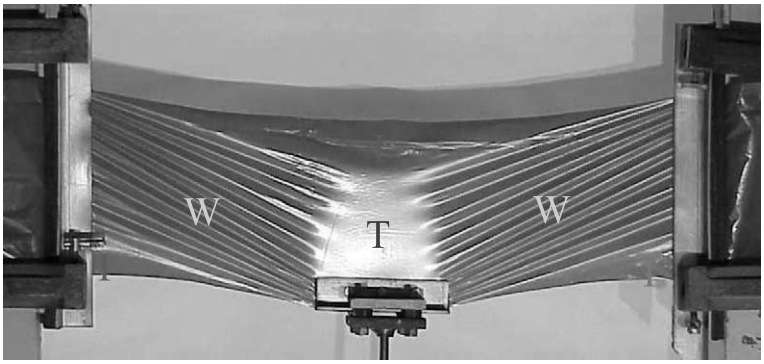

Fig. 1. Experimentally stretched rectangular membrane showing taut (T), wrinkled (W) and inactive (I) regions.

the applied loads is reversed, the body buckles locally, as it is unable to withstand any compression. In general, three different types of regions may appear in a stretched membrane. To illustrate, Fig. 1 represents a thin rectangular polyethylene sheet, laterally clamped and subjected to a uniform vertical displacement on the central portion of its base. Roughly speaking, some parts of the membrane are taut, that is, here a biaxial state of tensile stress is present. In other parts, wrinkling may develop, i.e., there is only one non-zero principal stress component, whose direction is indicated by the wrinkles. Finally, some other regions, like the upper upside-down triangle-shaped portion of the membrane, are completely buckled and consequently result inactive (or unstressed).

For our purposes, one peculiar consequence of the wrinkling phenomenon deserves remark: it can easily be observed that wrinkles do not develop randomly throughout the membrane, but rather, their location and orientation are, in fact, governed by a ''maximum stiffness criterion''. In other words, amongst all the possible wrinkle patterns that the membrane could develop to withstand the applied loads, it naturally (and ''intelligently'', we might add) assumes the one that maximizes its overall extensional stiffness (Wagner, 1929; Timoshenko and Gere, 1961). This can be intuitively inferred from the reasoning first set forth by Mansfield (1968). He observed that, because of the partial slackening, the state of stress in a wrinkled region would not change if, there, the membrane were cut along the direction of the wrinkles themselves. In fact, the loads are borne solely by tensile stresses acting precisely along the wrinkles, while, at right angles to them, the stress state is zero. Therefore, provided the cuts are made in the correct places and directions, the cut-membrane's overall response to the same boundary conditions that brought on the original wrinkle pattern will be the same as the intact one's. On the other hand, if the membrane were cut differently, the final stress state would differ from that of the intact one because the cuts are now incompatible with such a state.

These properties, described here as per (Mansfield, 1968) by simply relying upon intuition and experimental evidence, can be derived rigorously (Royer-Carfagni, 1999) in continuum-mechanics theories developed expressly to model wrinkling phenomenon (e.g. Tension Field Theory by Mansfield (1968)).

Such a noteworthy, ''optimal'', response suggested the idea of applying these theories to studying the behavior of an idealized ''web bridge'', whose deck is supported by an elastic membrane attached in various ways to lateral pylons. The results of such analysis, in turn, lead to considering a ''real bridge'', generally a cable-stayed one, in which the deck is suspended to the lateral pylons by a set of stays. The optimal arrangements for the real bridge stays can thus be inferred by examining the wrinkle patterns of the web-bridge membrane, in response to vertical loads acting upon its deck. The criterion adopted for this consists of the following. Obviously, no stays ought to be placed along the membrane's slack portions. Secondly, as it can be easily proved that, if the membrane's own weight is negligible, the wrinkles will be straight lines

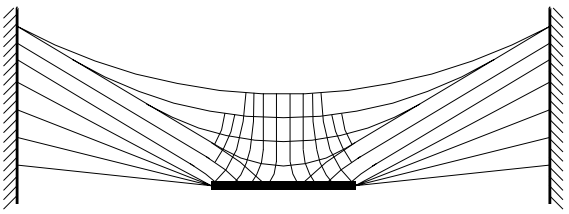

Fig. 2. Possible cable arrangement deduced from the trial in Fig. 1.

(Stein and Hedgepeth, 1961), it immediately follows that straight cables can be positioned along the wrinkle directions. Finally, the possible occurrence of taut regions suggests elements made up of by a net of cables, which we imagine as placed according to the lines of principal stress. For example, considering the rectangular-membrane layout in Fig. 1, where all the three different types of regions are present (taut, wrinkled and inactive), we would obtain the cable arrangement shown in Fig. 2.

In a recent paper (Royer-Carfagni, 1999), the case of a web bridge sustained by triangular-shaped membranes was analyzed. However, a number of approximations were introduced there: wrinkling was modeled using an approximate theory, specifically Tension Field Theory (Wagner, 1929; Reissner, 1938; Kondo, 1938; Kondo et al., 1955), accurate only for completely wrinkled membranes. Moreover, pylons were considered rigid and the bending stiffness of the deck was neglected. The aim of this paper is to develop a more comprehensive and exhaustive analysis, and the membrane model used here is, consequently, more extensive (Barsotti and Ligarò, 2000). In particular, *an ad* hoc version of the "relaxed strain energy", as proposed by Pipkin (1986), is presented in Section 2 in order to derive the correct equilibrium equations for plane infinitesimal wrinkly elasticity (see also Steigmann and Pipkin, 1989a,b; Steigmann, 1990). This approach has the considerable advantage that no a priori knowledge is required about the lines separating the different region types (taut, wrinkled or inactive) resulting at equilibrium. Each solution, represented by the stationary point of the modified (relaxed) total potential energy of the system, is found numerically by means of an expressly developed finite element code (Section 3).

Web bridges sustained by triangular-shaped membranes are considered in Section 4. Numerical analysis confirms that such membranes are wrinkled practically entirely, the corresponding wrinkle patterns being in good agreement with those previously deduced in (Royer-Carfagni, 1999). For different ratios of tower height to bridge length, what results from this unconventional approach are the classical fan, half-fan and harp patterns of cable-stayed bridges. However, by simply varying the membrane contours, more elaborate shapes may appear. In Section 5, we consider rectangular membranes, which instead generate all three different region types. By following the aforementioned criteria, we obtain cable arrangements that reveal remarkable similarities to some particular bridges, in which inclined stays collaborate with a suspension cable in carrying the applied loads. Recent studies have demonstrated the great stiffness of these structural schemes, which renders them particularly suitable for long-span railroad bridges.

2. The membrane model

Since the pioneering work by Wagner (1929), many attempts have been made to develop a theory of wrinkle elasticity. A main difficulty of modeling consists in the fact that, as is simply confirmed by stretching a swatch of cloth, even a very slight modification of the boundary conditions may produce appreciable differences in the wrinkle exact location and wavelength. However, if the membrane has sufficient extensional stiffness, some overall properties, such as the extent of the wrinkled regions and the direction of the wrinkles, are practically not affected. Since in most applications it is enough to consider

"smeared" wrinkles, many theories have been developed according to this line of reasoning, such as Mansfield's Tension field Theory (1968, 1970). However, in general, their range of application is limited to those particular cases where the body is completely wrinkled at equilibrium. Wu (1974) and Wu and Canfield (1981) advanced a more refined kinematical analysis, accounting for the possible co-existence of inactive, wrinkled and taut zones; but a difficulty in this approach is determining the location of the interfaces amongst the three different regions. A variational approach, inherently able to overcome this obstacle, was later proposed by Pipkin (1986) in the framework of finite elasticity theory. This formulation is very general, since only minimal assumptions for the membrane strain energy function, in particular its quasi-convexity, are needed. The shape of this function is then deduced theoretically, using functional analysis arguments.

Here, we propose an engineering approach to the same equilibrium problem, where the membrane is treated as a von Kàrmàn plate endowed with negligible bending stiffness. The corresponding (relaxed) strain energy is obtained applying Pipkin's fundamental ideas, but now strictly keeping to classical structural mechanics. It results a consistent linear-wrinkle-elasticity theory, particularly suitable for numerical implementation, which satisfactorily describes the behavior of membranes endowed with considerable extensional stiffness.

Consider a very thin membrane of constant thickness t, flat in its natural undistorted state and made of a homogeneous, linear-elastic, isotropic material, with Young's modulus E and Poisson's ratio v. Introduced a rectangular co-ordinate system (O,x,y,z), let $\Omega \subset \mathbb{R}^2$ represent the region of the (x,y) plane occupied by the membrane's mid-plane in its reference state. We denote u, v as the displacement components in the x and y directions, respectively, and w as the out-of-plane displacement. If $\Gamma \equiv \partial\Omega$ is the boundary of Ω, we assume that the planar displacement field, $u = \bar{u}$, $v = \bar{v}$, is assigned on a part Γ_u of Γ, whereas the in-plane edge-traction, $\bar{\mathbf{t}} = [\bar{t}_x, \bar{t}_y, 0]^{\mathrm{T}}$, acts on the remaining part, $\Gamma_t = \Gamma \setminus \Gamma_u$.

At equilibrium, because t is so small, we may assume that a generalized plane stress state predominates everywhere. Consequently, we neglect the displacement gradient in the z direction and consider $u = u(x,y)$, $v = v(x,y)$ and $w = w(x,y)$, where these quantities now present the through-the-thickness averaged values of the related displacement components. In the following analysis, we confine our attention to cases in which the membrane is highly stretched, but, because of the assumed considerable extensional stiffness, functions u and v, along with their derivatives, remain quite small everywhere. On the other hand, in wrinkled regions the transverse displacement w may experience high-frequency small-amplitude oscillations (Jenkins et al., 1998). Thus, in order to consider the possibility of large rotations associated to small planar displacements, we assume the von Kàrmàn's strain tensor as a suitable measure of deformation. Consequently, the relevant strain components take the form

$$\varepsilon_{xx} = \frac{\partial u}{\partial x} + \frac{1}{2}\left(\frac{\partial w}{\partial x}\right)^2, \quad \varepsilon_{yy} = \frac{\partial v}{\partial y} + \frac{1}{2}\left(\frac{\partial w}{\partial y}\right)^2, \quad 2\varepsilon_{xy} = \gamma_{xy} = \frac{\partial u}{\partial y} + \frac{\partial v}{\partial x} + \frac{\partial w}{\partial x}\frac{\partial w}{\partial y}, \tag{2.1}$$

whereas

$$\gamma_{xz} = 0, \quad \gamma_{yz} = 0, \quad \varepsilon_{zz} = -\frac{v}{1-v}(\varepsilon_{xx} + \varepsilon_{yy}). \tag{2.2}$$

A natural way exists to decompose the total strain (2.1). The quantities

$$\varepsilon^{\mathrm{p}}_{xx} = \frac{\partial u}{\partial x}, \quad \varepsilon^{\mathrm{p}}_{yy} = \frac{\partial v}{\partial y}, \quad 2\varepsilon^{\mathrm{p}}_{xy} = \gamma^{\mathrm{p}}_{xy} = \frac{\partial u}{\partial y} + \frac{\partial v}{\partial x}, \tag{2.3}$$

define the "planar strain tensor", $\boldsymbol{\varepsilon}^{\mathrm{p}}$, whereas the remaining part

$$\varepsilon^{\mathrm{w}}_{xx} = \frac{1}{2}\left(\frac{\partial w}{\partial x}\right)^2, \quad \varepsilon^{\mathrm{w}}_{yy} = \frac{1}{2}\left(\frac{\partial w}{\partial y}\right)^2, \quad 2\varepsilon^{\mathrm{w}}_{xy} = \frac{\partial w}{\partial x}\frac{\partial w}{\partial y}, \tag{2.4}$$

due to the out-of-plane component w only, can be related to the wrinkle strain tensor, $\boldsymbol{\varepsilon}^{\mathrm{w}}$, proposed by Wu (1974). We observe in passing that, since in Eq. (2.4) $\varepsilon^{\mathrm{w}}_{xx}\varepsilon^{\mathrm{w}}_{yy} - (\varepsilon^{\mathrm{w}}_{xy})^2 = 0$, the strain state associate to Eq. (2.4) is rank-one.

According to the aforementioned assumptions, we consider the membrane as a von Kàrmàn's plate with negligible bending stiffness. Consequently, its strain energy reduces to the extensional contribution

$$U(\boldsymbol{\varepsilon}) = \frac{Et}{2(1-\nu^2)}\left(\varepsilon^2_{xx} + \varepsilon^2_{yy} + 2\nu\varepsilon_{xx}\varepsilon_{yy} + \frac{1+\nu}{2}\varepsilon^2_{xy}\right). \tag{2.5}$$

Using the decomposition, $\boldsymbol{\varepsilon} = \boldsymbol{\varepsilon}^{\mathrm{p}} + \boldsymbol{\varepsilon}^{\mathrm{w}}$, and following Pipkin's ideas, a relaxed strain energy for the plate can be defined. For any constant symmetric tensor $\boldsymbol{\varepsilon}^{\mathrm{p}}$, we set

$$U_{\mathrm{rel}}(\boldsymbol{\varepsilon}^{\mathrm{p}}) = \frac{1}{A(\omega)}\inf_{\boldsymbol{\varepsilon}^{\mathrm{w}}}\int_{\omega} U(\boldsymbol{\varepsilon}^{\mathrm{p}} + \boldsymbol{\varepsilon}^{\mathrm{w}})\,\mathrm{d}a. \tag{2.6}$$

Here, the infimum is to be taken for all bounded subsets $\omega \subset \Omega$ of area $A(\omega)$, and for all symmetric positive semi-definite tensors $\boldsymbol{\varepsilon}^{\mathrm{w}}$ of the type (2.4). Such definition is remindful, in our model, of the quasiconvexity condition of Morrey (1952). The function U_{rel} automatically accounts for the well-known property of the membranes, i.e. the wrinkle strain $\boldsymbol{\varepsilon}^{\mathrm{w}}$ "smartly" tends to accommodate the planar deformation in order to lower the energy, wherever possible.

The expression (2.6) can be conveniently written by selecting the reference axes parallel to the principal direction of the tensor $\boldsymbol{\varepsilon}^{\mathrm{p}}$. Indicating with $\varepsilon^{\mathrm{p}}_1$ and $\varepsilon^{\mathrm{p}}_2$ its principal components, Eq. (2.5) becomes

$$U(\boldsymbol{\varepsilon}) = U(\boldsymbol{\varepsilon}^{\mathrm{p}} + \boldsymbol{\varepsilon}^{\mathrm{w}}) = \frac{Et}{2(1-\nu^2)}\left[(\varepsilon^{\mathrm{p}}_1 + \varepsilon^{\mathrm{w}}_{11})^2 + (\varepsilon^{\mathrm{p}}_2 + \varepsilon^{\mathrm{w}}_{22})^2 + 2\nu(\varepsilon^{\mathrm{p}}_1 + \varepsilon^{\mathrm{w}}_{11})(\varepsilon^{\mathrm{p}}_2 + \varepsilon^{\mathrm{w}}_{22}) + \frac{1+\nu}{2}(\varepsilon^{\mathrm{w}}_{12})^2\right],$$

$\varepsilon^{\mathrm{w}}_{11}$, $\varepsilon^{\mathrm{w}}_{22}$ and $\varepsilon^{\mathrm{w}}_{12}$ being the components of the wrinkle strain tensor $\boldsymbol{\varepsilon}^{\mathrm{w}}$ in the same reference system. Now, in order to lower the energy, it is always convenient to choose $\varepsilon^{\mathrm{w}}_{12} = 0$, which means that $\boldsymbol{\varepsilon}^{\mathrm{p}}$ and $\boldsymbol{\varepsilon}^{\mathrm{w}}$ must be coaxial. Thus, indicating with $\varepsilon^{\mathrm{w}}_1$ and $\varepsilon^{\mathrm{w}}_2$ the corresponding principal values of the wrinkle strain tensor $\boldsymbol{\varepsilon}^{\mathrm{w}}$, we find

$$U(\boldsymbol{\varepsilon}) = \frac{Et}{2(1-\nu^2)}[(\varepsilon^{\mathrm{p}}_1 + \varepsilon^{\mathrm{w}}_1)^2 + (\varepsilon^{\mathrm{p}}_2 + \varepsilon^{\mathrm{w}}_2)^2 + 2\nu(\varepsilon^{\mathrm{p}}_1 + \varepsilon^{\mathrm{w}}_1)(\varepsilon^{\mathrm{p}}_2 + \varepsilon^{\mathrm{w}}_2)]. \tag{2.7}$$

Because of the symmetry of formula (2.7), without loosing generality, we discuss the case in which $\varepsilon^{\mathrm{p}}_1 \geqslant \varepsilon^{\mathrm{p}}_2$. Thus, supposing ω sufficiently regular, we distinguish two possibilities.

(i) Assume $\varepsilon^{\mathrm{p}}_1 < 0$. In the most general case, despite of the rank-one character of $\boldsymbol{\varepsilon}^{\mathrm{w}}$, we may determine (see e.g., Bhattacharya and Dolzmann, 2000) a sequence of piecewise-constant rank-one deformation fields (representative, e.g., of a diamond-shaped bulging), (weakly) converging to a positive definite deformation field $\hat{\varepsilon}^{\mathrm{w}}$ such that $\hat{\varepsilon}^{\mathrm{w}}_1 = -\varepsilon^{\mathrm{p}}_1$ and $\hat{\varepsilon}^{\mathrm{w}}_2 = -\varepsilon^{\mathrm{p}}_2$. Consequently, we obtain $U_{\mathrm{rel}} = 0$.
(ii) Assume instead $\varepsilon^{\mathrm{p}}_1 \geqslant 0$. The minimum of Eq. (2.7) is clearly obtained when $\varepsilon^{\mathrm{w}}_1 = 0$ and $\varepsilon^{\mathrm{p}}_2 + \varepsilon^{\mathrm{w}}_2 = -\nu\varepsilon^{\mathrm{p}}_1$. But, since $\varepsilon^{\mathrm{w}}_2 \geqslant 0$ in Eq. (2.4), we can satisfy this condition only when $\varepsilon^{\mathrm{p}}_2 < -\nu\varepsilon^{\mathrm{p}}_1$. If this is the case, we find $U_{\mathrm{rel}}(\varepsilon^{\mathrm{p}}_1, \varepsilon^{\mathrm{p}}_2) = Et(\varepsilon^{\mathrm{p}}_1)^2/2$. Otherwise, we cannot do any better but selecting $\varepsilon^{\mathrm{w}}_1 = \varepsilon^{\mathrm{w}}_2 = 0$ and obtain $U_{\mathrm{rel}}(\varepsilon^{\mathrm{p}}_1, \varepsilon^{\mathrm{p}}_1) = Et\lfloor(\varepsilon^{\mathrm{p}}_1)^2 + (\varepsilon^{\mathrm{p}}_2)^2 + 2\nu\varepsilon^{\mathrm{p}}_1\varepsilon^{\mathrm{p}}_2\rfloor/2(1-\nu^2)$.

We observe that, using the relaxed energy concept, we may analyze the equilibrium state of a membrane independently of any knowledge of the field w. Indeed, in this theory, w remains undetermined, but the effects of wrinkling and buckling are implicitly considered in the definition (2.6).

The physical interpretation of this finding is immediate. We classify portions of the membrane respectively as taut, wrinkled or inactive (i.e., slack) provided that the point representative of their planar strain

state belongs to one of the three regions T, $W = W_1 \cup W_2$ or I, defined in the principal-strain plane $(O, \varepsilon_1^p, \varepsilon_2^p)$ as

$$T := \left\{(\varepsilon_1^p, \varepsilon_2^p) \in \mathbb{R}^2 \ \middle| \ \varepsilon_1^p \geqslant -\nu\varepsilon_2^p \text{ and } \varepsilon_2^p \geqslant -\nu\varepsilon_1^p\right\}, \tag{2.8a}$$

$$W_1 := \left\{(\varepsilon_1^p, \varepsilon_2^p) \in \mathbb{R}^2 \ \middle| \ \varepsilon_1^p \geqslant 0 \text{ and } \varepsilon_2^p < -\nu\varepsilon_1^p\right\}, \tag{2.8b}$$

$$W_2 := \left\{(\varepsilon_1^p, \varepsilon_2^p) \in \mathbb{R}^2 \ \middle| \ \varepsilon_2^p \geqslant 0 \text{ and } \varepsilon_1^p < -\nu\varepsilon_2^p\right\}, \tag{2.8c}$$

$$I := \left\{(\varepsilon_1^p, \varepsilon_2^p) \in \mathbb{R}^2 \ \middle| \ \varepsilon_1^p < 0 \text{ and } \varepsilon_2^p < 0\right\}. \tag{2.8d}$$

Such regions are depicted in Fig. 3, which represents a linear version of the domain considered in (Pipkin, 1986). Expressions (2.8a)–(2.8d) can be easily interpreted introducing the natural (transverse) contraction of the membrane, which is the linear form of the natural width concept proposed by Pipkin in finite elasticity. For a strip of membrane, homogeneous and isotropic, under uniaxial tensile stress σ_1, the natural contraction is defined as $\varepsilon_2 = -\nu\varepsilon_1$, where $\varepsilon_1 = \sigma_1/E$ is the principal tensile strain.

Therefore, the relaxed strain energy may be written in the following form:

$$U_{\text{rel}}(\varepsilon_1^p, \varepsilon_2^p) := \frac{Et}{2}\begin{cases} 0 & \text{if } (\varepsilon_1^p, \varepsilon_2^p) \in I \\ (\varepsilon_1^p)^2 & \text{if } (\varepsilon_1^p, \varepsilon_2^p) \in W_1 \\ (\varepsilon_2^p)^2 & \text{if } (\varepsilon_1^p, \varepsilon_2^p) \in W_2 \\ \dfrac{(\varepsilon_1^p)^2 + (\varepsilon_2^p)^2 + 2\nu\varepsilon_1^p\varepsilon_2^p}{1-\nu^2} & \text{if } (\varepsilon_1^p, \varepsilon_2^p) \in T \end{cases}. \tag{2.9}$$

It follows that in a taut region T, the state of stress is biaxial and takes the form

$$\sigma_1 = \frac{\partial U_{\text{rel}}}{\partial \varepsilon_1^p} = \frac{E}{1-\nu^2}(\varepsilon_1^p + \nu\varepsilon_2^p) \geqslant 0, \quad \sigma_2 = \frac{\partial U_{\text{rel}}}{\partial \varepsilon_2^p} = \frac{E}{1-\nu^2}(\varepsilon_2^p + \nu\varepsilon_1^p) \geqslant 0. \tag{2.10}$$

Both components are non-negative because, from (2.8a), we have $\varepsilon_1^p \geqslant -\nu\varepsilon_2^p$ and $\varepsilon_2^p \geqslant -\nu\varepsilon_1^p$. Considering the wrinkled region W_1 where $\varepsilon_1^p \geqslant 0$, we find

$$\sigma_1 = \frac{\partial U_{\text{rel}}}{\partial \varepsilon_1^p} = E\varepsilon_1^p \geqslant 0 \quad \text{and} \quad \sigma_2 = \frac{\partial U_{\text{rel}}}{\partial \varepsilon_2^p} = 0. \tag{2.11}$$

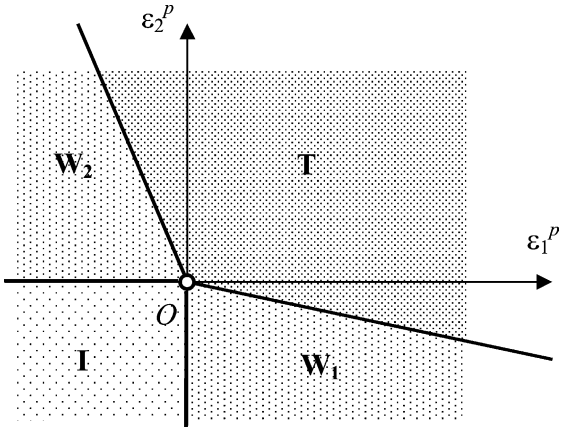

Fig. 3. The three different types of membrane states in the $(O, \varepsilon_1^p, \varepsilon_2^p)$ plane.

Analogously in W_2, where $\varepsilon_2^{\mathrm{p}} \geqslant 0$, we obtain $\sigma_1 = 0$ and $\sigma_2 = E\varepsilon_2^{\mathrm{p}} \geqslant 0$. Finally, within the inactive region I, it is a simple matter to show that $\sigma_1 = \sigma_2 = 0$.

Thus, the peculiarity of Eq. (2.9) is that compressive stresses never appear in the membrane. Buckling and wrinkling phenomena are formally treated as a physical, rather than a geometrical, non-linearity. In other words, the planar strain (2.3) becomes the only significant measure of deformation, since the wrinkling effects described by Eq. (2.4) are automatically considered through the strain energy density (2.9).

3. The solution procedure

In the following, for simplicity's sake, we will omit the superscript 'p' in the expressions for planar strains (2.3). For numerical implementation, it is necessary to derive the explicit expressions for the rectangular stress components σ_{xx}, σ_{yy}, and τ_{xy} within each different region. Thus, since from the chain rule

$$\sigma_{ij} = \sum_{k=1}^{2} \frac{\partial U_{\mathrm{rel}}}{\partial \varepsilon_k} \frac{\partial \varepsilon_k}{\partial \varepsilon_{ij}}, \tag{3.1}$$

we obtain in a taut region T

$$\sigma_{xx} = \frac{E}{1-\nu^2}(\varepsilon_{xx} + \nu\varepsilon_{yy}), \quad \sigma_{yy} = \frac{E}{1-\nu^2}(\varepsilon_{yy} + \nu\varepsilon_{xx}), \quad \tau_{xy} = \frac{E}{1+\nu}\gamma_{xy}. \tag{3.2}$$

When considering the wrinkled regions, without loosing generality, we may assume $\varepsilon_1 \geqslant \varepsilon_2$, so that W_2 is never attained. Thus, introducing $r = \sqrt{(\varepsilon_{xx} - \varepsilon_{yy})^2 + \gamma_{xy}^2}/2$, we find in the whole wrinkled region W

$$\sigma_{xx} = \frac{E\varepsilon_1}{2}\left[1 + \frac{\varepsilon_{xx} - \varepsilon_{yy}}{2r}\right] = \sigma_1 \cos^2\alpha, \quad \sigma_{yy} = \frac{E\varepsilon_1}{2}\left[1 - \frac{\varepsilon_{xx} - \varepsilon_{yy}}{2r}\right] = \sigma_1 \sin^2\alpha,$$

$$\tau_{xy} = \frac{E\varepsilon_1}{2}\frac{\gamma_{xy}}{2r} = \sigma_1 \sin\alpha\cos\alpha, \tag{3.3}$$

where, as per (Mansfield, 1968), α is the angle that the tensile principal direction 1 forms with the x-axis. We observe, in passing, that these formulas for stress in wrinkled regions coincide with those obtained by Stein and Hedgepeth (1961). Finally, within the inactive region I, we have $\sigma_{xx} = 0$, $\sigma_{yy} = 0$, and $\tau_{xy} = 0$.

The expressions above can be more concisely written as $\boldsymbol{\sigma} = \mathbf{D}_{\mathrm{rel}}\boldsymbol{\varepsilon}$, where $\boldsymbol{\sigma} = \left[\sigma_{xx}, \sigma_{yy}, \tau_{xy}\right]^{\mathrm{T}}$, $\boldsymbol{\varepsilon} = \left[\varepsilon_{xx}, \varepsilon_{yy}, \gamma_{xy}\right]^{\mathrm{T}}$, and $\mathbf{D}_{\mathrm{rel}}$ is one of the following matrices

$$\mathbf{D}_{\mathrm{rel}}^{\mathrm{T}} = \mathbf{D}_{\mathrm{el}} = \frac{E}{1-\nu^2}\begin{bmatrix} 1 & \nu & 0 \\ \nu & 1 & 0 \\ 0 & 0 & 1-\nu \end{bmatrix} \text{ in } T, \tag{3.4a}$$

$$\mathbf{D}_{\mathrm{rel}}^{W} = \frac{E}{2}\begin{bmatrix} 1 + ((\varepsilon_{xx} - \varepsilon_{yy})/2r) & 0 & \gamma_{xy}/4r \\ 0 & 1 + ((\varepsilon_{yy} - \varepsilon_{xx})/2r) & \gamma_{xy}/4r \\ \gamma_{xy}/4r & \gamma_{xy}/4r & 1/2 \end{bmatrix} \text{ in } W, \tag{3.4b}$$

$$\mathbf{D}_{\mathrm{rel}}^{I} = \mathbf{0} \text{ in } I. \tag{3.4c}$$

These formulas clearly evidence the stress dependence of the material's extensional stiffness already pointed out by Reissner (1938) and Mansfield (1968, 1970). As a consequence, the problem of finding the equilibrium state of a partially wrinkled membrane is always highly non-linear.

With the aim of using a FEM analysis, the entire region $\Omega \subset \mathbb{R}^2$ is divided into a set of M plane isoparametric elements, ω_m, $m = 1, \ldots, M$, either triangular or quadrilateral in shape. Assuming bilinear interpolation, for any given element we consider the displacement field

$$u(x,y) = \mathbf{N}(x,y) \cdot \mathbf{u}, \quad v(x,y) = \mathbf{N}(x,y) \cdot \mathbf{v}, \tag{3.5}$$

where $\mathbf{N}(x,y)$ is the vector collecting the interpolation functions, while the vectors $\mathbf{u}$ and $\mathbf{v}$ contain the nodal displacement components in the x and y directions, respectively. The strain–displacement relations become

$$\boldsymbol{\varepsilon} = \begin{bmatrix} \varepsilon_x \\ \varepsilon_y \\ \gamma_{xy} \end{bmatrix} = \begin{bmatrix} \partial \mathbf{N}^{\mathrm{T}}/\partial x & \mathbf{0}^{\mathrm{T}} \\ \mathbf{0}^{\mathrm{T}} & \partial \mathbf{N}^{\mathrm{T}}/\partial y \\ \partial \mathbf{N}^{\mathrm{T}}/\partial y & \partial \mathbf{N}^{\mathrm{T}}/\partial x \end{bmatrix} \begin{bmatrix} \mathbf{u} \\ \mathbf{v} \end{bmatrix} = \mathbf{B} \begin{bmatrix} \mathbf{u} \\ \mathbf{v} \end{bmatrix}, \tag{3.6}$$

so that the $2N \times 2N$ stiffness matrix for the mth element results to be

$$\mathbf{k}_m = \int_{\omega_m} \mathbf{B}^{\mathrm{T}} \mathbf{D}^m_{\mathrm{rel}} \mathbf{B} \, \mathrm{d}\omega. \tag{3.7}$$

Here, $\mathbf{D}^m_{\mathrm{rel}}$, assumed constant within each element, is one of the three 3×3 material-stiffness matrices defined in Eqs. (3.4a)–(3.4c). In other words, the whole region covered by a single finite element is considered to be entirely either taut or wrinkled or inactive. It follows that the serrated line, defined by element boundaries, numerically approximates the interfaces between the different regions.

Indicating with $\mathbf{q}$ the vector collecting all the nodal displacements of the planar model, the governing set of equilibrium equations is given by the stationary conditions for the functional

$$\Pi(\mathbf{q}) = U_{\mathrm{rel}}(\mathbf{q}) - P(\mathbf{q}), \tag{3.8}$$

representing the total potential energy of the system. Now $U_{\mathrm{rel}}(\mathbf{q})$ indicates the relaxed strain energy derived from Eq. (2.9), while $P(\mathbf{q})$ represents the work of the external loads. Finding the stationary points of Eq. (3.8) corresponds to solving the non-linear system of equations

$$\frac{\partial \Pi}{\partial \mathbf{q}} = \mathbf{K}(\mathbf{q})\mathbf{q} - \mathbf{p} = 0, \tag{3.9}$$

where $\mathbf{K}(\mathbf{q}) = \sum_m \mathbf{k}_m(\mathbf{q})$ is the unknown secant stiffness matrix of the system and $\mathbf{p} = \partial P/\partial \mathbf{q}$ is the vector of the external nodal loads. Proper boundary conditions need to be added.

The choice of the most convenient numerical procedure is based on the following observations.

The nature of the problem advises against the use of incremental methods, since the main unknowns (i.e., the separation lines between inactive, wrinkled and taut regions) depend upon the distribution and shape of the applied loads, rather than upon their magnitude. In other words, if the loads were incremented proportionally to the same parameter, the state of stress would be proportionally increased, but the location of inactive, wrinkled and taut regions would be unaffected.

For the same reason, incremental-iterative methods (path-following strategies), using tangent-stiffness matrices, may fail if, during the iterative process, some nodes turn out to be surrounded by elements of inactive regions. In this case, in fact, the tangent-stiffness matrix becomes irremediably singular. Therefore, numerical algorithms based upon Newton–Raphson schemes fail as soon as such a situation occurs (Roddeman et al., 1987a,b; Kang and Im, 1997).

In order to solve the non-linear system (3.9), a modified Newton–Raphson strategy has instead proved to be effective. Denoting with $\mathbf{K}_{\mathrm{el}}$ the global stiffness matrix corresponding to the ideal case in which the membrane is taut everywhere, obtained through assemblage of matrices of the type (3.4a), we can write Eq. (3.9) in the form

$$\mathbf{K}_{\mathrm{el}}\mathbf{q} = (\mathbf{K}_{\mathrm{el}} - \mathbf{K}(\mathbf{q}))\mathbf{q} + \mathbf{p}. \tag{3.10}$$

From this, we derive the iterative scheme

$$\mathbf{q}^{(n)} = \mathbf{q}^{(n-1)} + \mathbf{K}_{\mathrm{el}}^{-1}\left[\mathbf{p} - \mathbf{K}(\mathbf{q}^{(n-1)})\mathbf{q}^{(n-1)}\right]. \tag{3.11}$$

At cycle n, the secant stiffness matrix $\mathbf{K}(\mathbf{q}^{(n-1)})$ is obtained from assembling the elemental stiffness matrices (3.4a)–(3.4c), which are selected element-wise, according to the criterion (2.8a)–(2.8d), for the values $\mathbf{q} = \mathbf{q}^{(n-1)}$. In other words, we find out which elemental matrix to use at cycle n from the planar strains obtained at cycle $n-1$.

The procedure (3.11) has considerable advantages. Not only is just one matrix inversion required, but also, what is more important, the secant matrix $\mathbf{K}(\mathbf{q}^{(n-1)})$, which may be singular, is never inverted. Roughly speaking, the strategy consists in regarding the membrane as a plate, where tensile stresses may coexist with compressive ones. In order to avoid this inconsistency, at cycle n we add to the real load $\mathbf{p}$ the relaxing system of loads $-\mathbf{K}(\mathbf{q}^{(n-1)})\mathbf{q}^{(n-1)}$. The magnitude of these loads is selected such to annihilate any compressive stress active in the membrane at cycle $n-1$. The accuracy of this procedure may continuously be checked by evaluating the term $\left|\mathbf{p} - \mathbf{K}(\mathbf{q}^{(n-1)})\mathbf{q}^{(n-1)}\right|$, which indicates the "compression level" still present in the membrane at the current stage. Convergence is achieved when

$$\left|\mathbf{q}^{(n)} - \mathbf{q}^{(n-1)}\right| \leqslant \mathrm{Tol}, \tag{3.12}$$

where $\mathrm{Tol} > 0$ is a chosen tolerance.

The inclusion in the model of linear-elastic beam elements to simulate the deck and pylons is straightforward provided that compatibility between beams and membrane elements is guaranteed. This is obtained by requiring that displacements of common nodes to be equal, thus allowing the possibility of relative rotation.

In Fig. 4a we represent the stress distribution for a membrane in the configuration of Fig. 1. The state of stress is graphically represented by small crosses oriented according to the principal directions, with the lengths of their arms drawn in a suitably proportional scale to the value of the principal components. In this

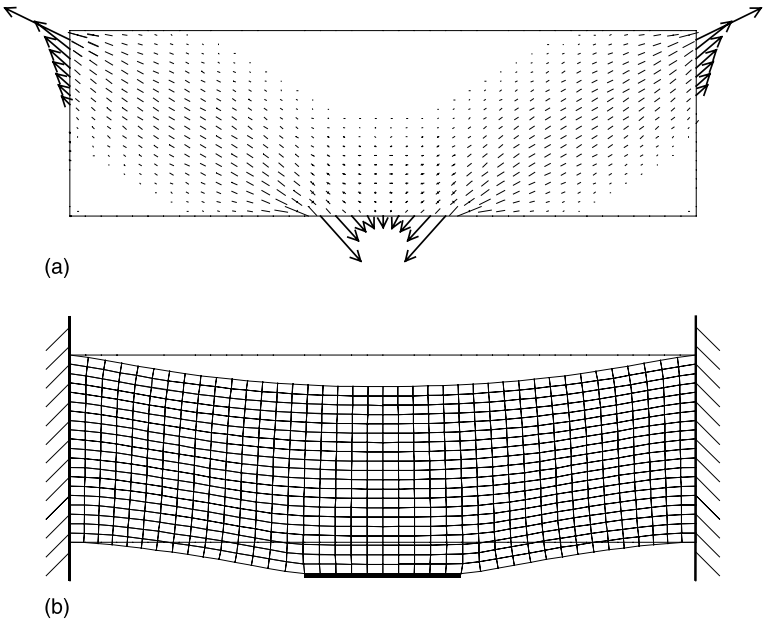

Fig. 4. (a) Membrane stress distribution and (b) deformed shape for the same boundary conditions as for the test in Fig. 1.

way, those points where the membrane remains inactive can be easily recognized by the disappearance of both arms of the cross. Moreover, in wrinkled regions the cross reduces to a single segment oriented according to the only non-vanishing principal stress. In Fig. 4b, we also report the deformed shape of the membrane. The effectiveness of the numerical procedure is confirmed by comparing the experimental results of Fig. 1. with the numerical simulation represented in Fig. 4.

4. Triangular membranes

The parameters that influence the equilibrium state of a web bridge are numerous. Different kinds of wrinkle patterns are obtained by simply varying the ratio between pylon height H and bridge length L, and even more so, by altering the initial shape of the elastic membrane. In order to address the various possible situations systematically, we begin, as a first approximation, by neglecting the deformation of the pylons. Thus, we consider the case in which two right-angled triangular membranes, clamped on the vertical side and free on the oblique sides, are connected to a flexible beam on their horizontal edge, according to the scheme of Fig. 5. For convenience, and without loosing generality, we consider the case in which both the membranes and the beam are made of the same homogeneous, elastic, isotropic material, for which we set $E = 2.1 \times 10^5$ MPa and $\nu = 0.1$. Our aim is to find the equilibrium state of the system when a uniformly distributed vertical load q acts on the deck, represented by the horizontal beam. Four parameters will be considered as variables in the analysis: the height of the pylons H, the clear span of the bridge L, the thickness of the membrane t, and the moment of inertia J_d of the deck's cross-section. It may be worthwhile to recall that when body forces are negligible, the lines of the non-zero principal stress are straight (hence Wagner's denomination of tension rays (Mansfield, 1968)) and coincide with the direction of the wrinkles in the membrane.

The situation described in Fig. 5 is similar to that discussed in Royer-Carfagni (1999), where an approximate explicit solution was found for the borderline case of an extremely flexible beam ($J_d \to 0$). Under this approximation, the membrane results completely wrinkled. In order to make comparisons between the results obtained therein and this more accurate numerical analysis, we shall assume $t = 1$ cm and a very small deck inertia ($J_d = 0.01$ m^4). We then consider four different situations, corresponding to the ratios $H/L = 0.25$, 0.5, 1, and 2. The resulting stress distributions are reported in Fig. 6, where the reaction forces of the pylons have also been illustrated. In this situation, according to our expectation, the membrane turns out to be practically completely wrinkled.

In order to design a real bridge according to the criteria presented in the Introduction, we consider the cable arrangement obtained by placing cables along the tension rays. By selecting those rays whose intersection points with the horizontal beam are nearly equidistant, we obtain the schemes reported in Fig. 7,

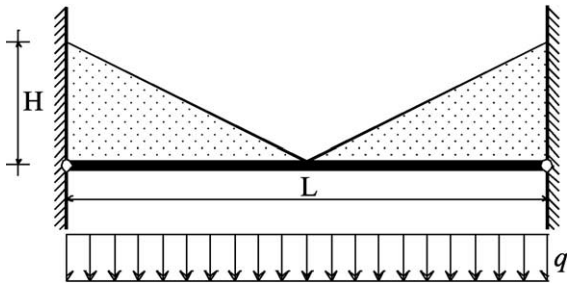

Fig. 5. Static scheme for a web bridge with triangular membranes and rigid pylons.

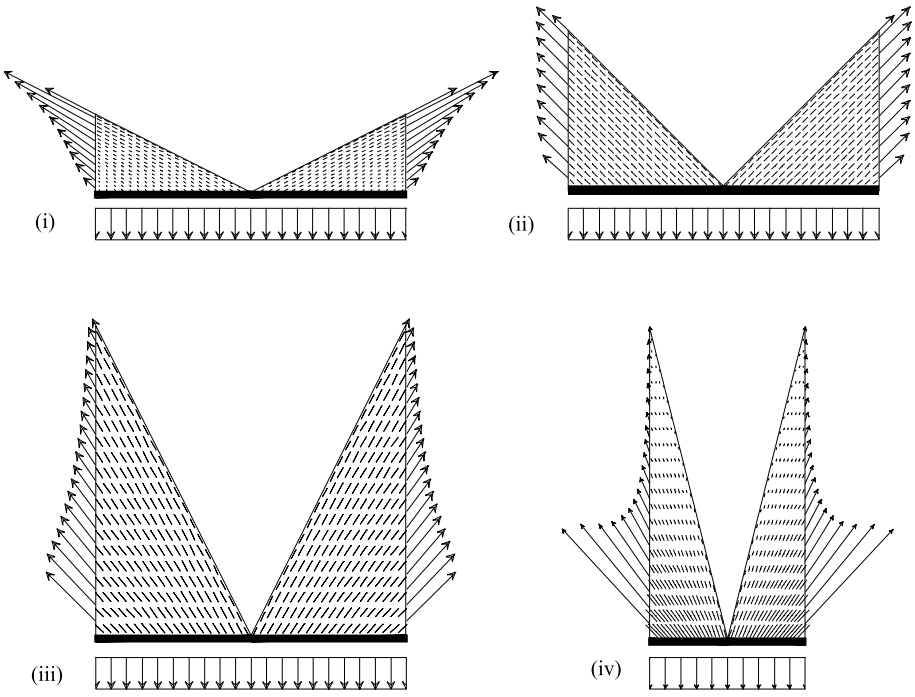

Fig. 6. Influence of the ratio H/L on the stress distribution within the membrane. $L = 100$ m, $J_d = 0.01$ m^4, $t = 1$ cm. (i) $H/L = 0.25$, (ii) $H/L = 0.5$, (iii) $H/L = 1$ and (iv) $H/L = 2$.

which reproduce the classical arrangements of cable-stayed bridges. More in particular, when $H/L = 0.5$, the membranes are half squares, and the tension rays tend to become almost parallel, resembling the classical harp pattern. As the ratio between the pylon height and bridge clear span is reduced, the rays tend to converge at the upper vertex, thus reproducing the traditional half-fan scheme (see case i) in Fig. 6.

It should be clear from Fig. 6(iv) that when the height of the membrane is greater than its length ($H/L > 1$), its uppermost parts result only slightly stressed, suggesting that these portions play a secondary role in sustaining the applied loads. In other words, increasing the height of the pylons beyond a certain limit is unlikely to produce any appreciable increase in the bridge stiffness. In order to delve into this point further, let us introduce the quantity

$$\kappa = \frac{q^2 L^2}{2tEU_{\mathrm{rel}}} \tag{4.1}$$

where U_{rel} represents the strain energy stored in the membrane. Clearly, κ is dimensionless, and the greater its value, the greater will be the average stiffness of the web bridge. In Fig. 8, κ is plotted as a function of H/L for fixed $L = 100$ m, $t = 1$ cm and $J_d = 0.1$ m^4. The graph exhibits a horizontal asymptote for large H/L, a finding that confirms our conjecture that the material is not fully exploited by increasing the height of the pylons beyond a certain limit.

More in detail, we may consider the specific average stiffness, κ^*, defined as

$$\kappa^* = \frac{\kappa}{A} = \frac{q^2 L^2}{2tEAU_{\mathrm{rel}}} \tag{4.2}$$

where A represents the total area of the membrane. The graph of κ^*, reported in Fig. 9, reaches a maximum at $H/L = 0.5$, suggesting this as the optimal ratio between pylon height and bridge length.

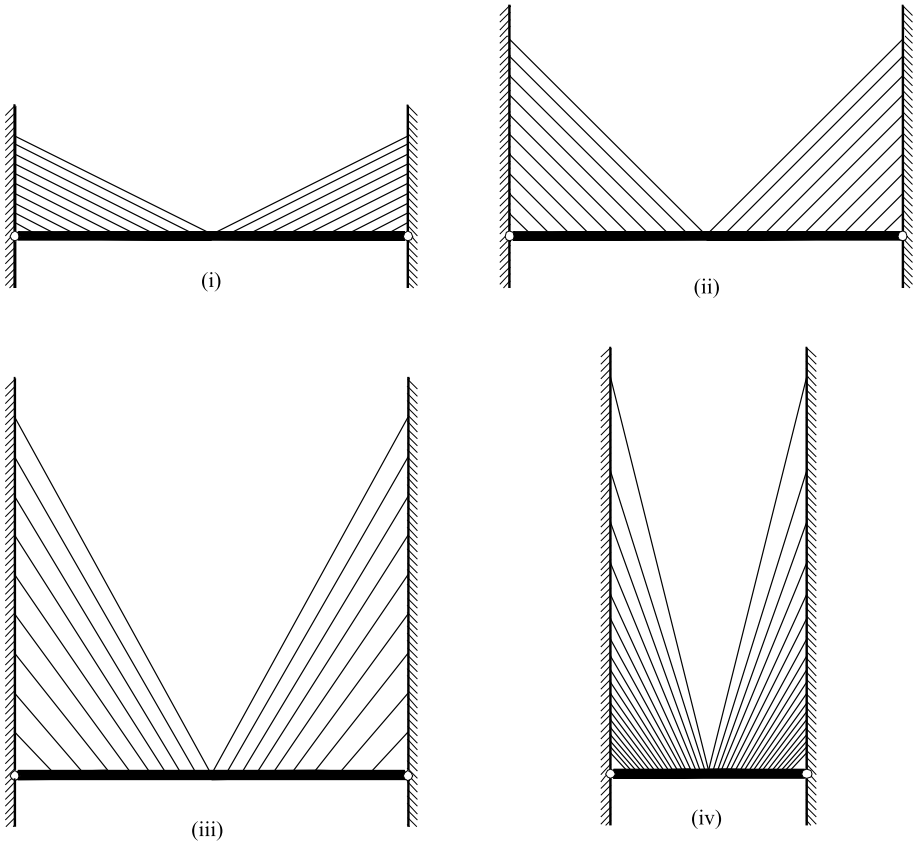

Fig. 7. Various stay arrangements resulting from the cases in Fig. 6. (i) $H/L = 0.25$, (ii) $H/L = 0.5$, (iii) $H/L = 1$ and (iv) $H/L = 2$.

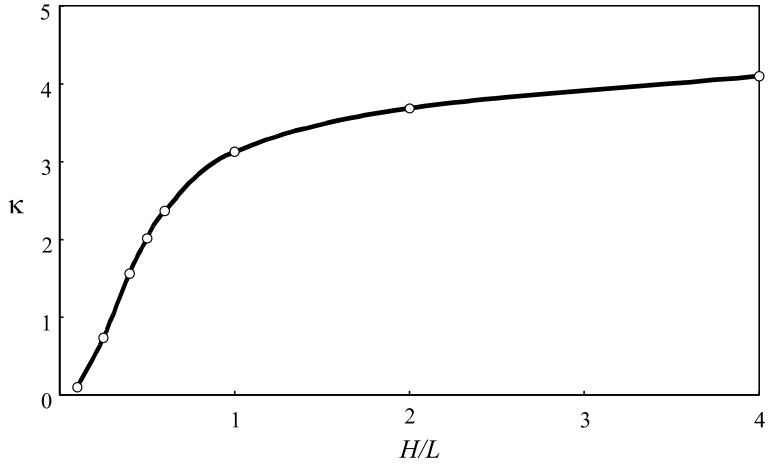

Fig. 8. Average stiffness κ of the web bridge as a function of the ratio H/L for varying H and fixed $L = 100$ m, $t = 1$ cm, $J_d = 0.1$ m^4. Loads are considered uniformly distributed on the deck.

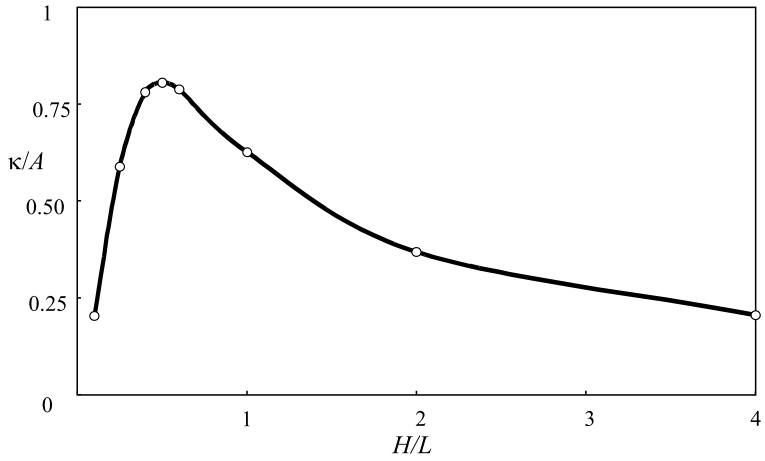

Fig. 9. Specific average stiffness κ^* of the web bridge as a function of the ratio H/L for $L = 100$ m, $t = 1$ cm, $J_d = 0.1$ m^4. Loads are considered uniformly distributed on the deck.

In the foregoing cases, the bending stiffness of the deck is very small in comparison to that offered by the membrane. Other numerical simulations have shown that the wrinkle pattern is practically unaffected by varying the beam inertia. In rough terms, the wrinkle pattern depends upon the shape rather than the amplitude of the inflection line of the beam, which is only marginally influenced by the inertia of the cross-section. However, the stress state in the membrane changes significantly because the stiffer the beam, the greater is the load portion it sustains.

We now turn to the slightly different situation in which the membrane is partially disconnected from the pylons and/or the beam (Fig. 10). This case aims to represent those circumstances in which, due to some design requirement, the stays cannot be connected to some portions of the pylons and/or deck. With the same notation as Fig. 10, Fig. 11 refers to different H_1/H and L_1/L ratios. Predictably, the presence of cuts now constrains the pattern of the tensions rays which, for $H_1/H \to 1$, resembles the classical fan pattern of a cable stayed bridge. Moreover, membrane portions, in proximity of the disconnected sides, remain practically inactive.

The stay arrangements that can be obtained from the cases considered in Fig. 11 are illustrated in Fig. 12. If stays were placed according to the resulting tension-ray pattern, the classical half-fan arrangement would result.

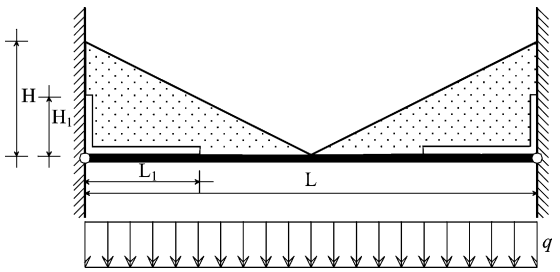

Fig. 10. A membrane partially disconnected from pylons and/or deck. Case $H/L = 0.25$.

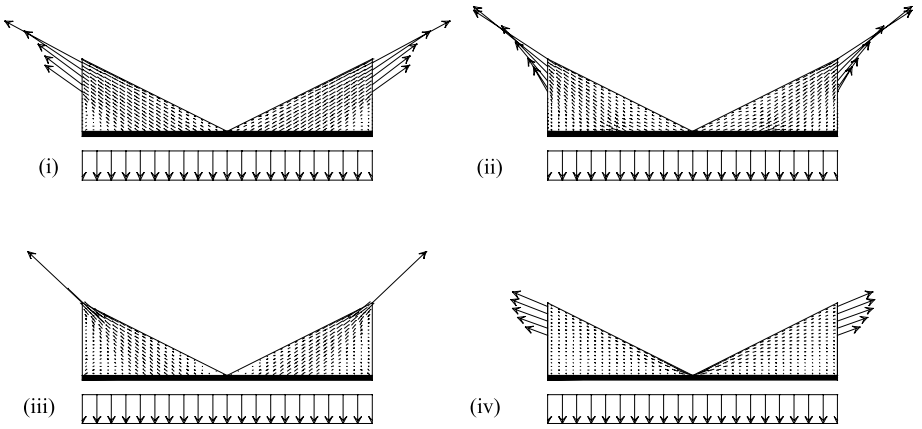

Fig. 11. Membrane equilibrium states when partially disconnected. Case $H/L = 0.25$, $L = 100$ m, $t = 1$ cm, $J_d = 15.5$ m^4. (i) $H_1/H = 0.5$ and $L_1/L = 0$, (ii) $H_1/H = 0.5$ and $L_1/L = 0.25$, (iii) $H_1/H = 1.0$ and $L_1/L = 0$, (iv) $H_1/H = 0.5$ and $L_1/L = 0.5$.

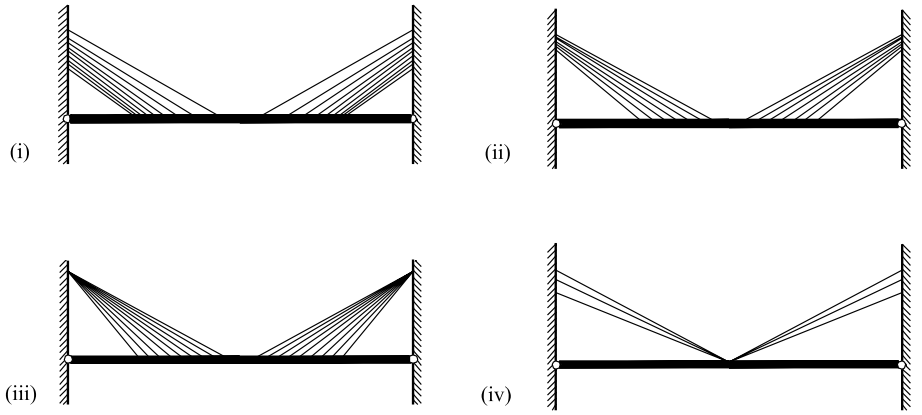

Fig. 12. Cable arrangements resulting from partial disconnection of the membranes from pylons and deck. Same cases as in Fig. 11.

The case $L_1/L \to 0.50$ is representative of a pin-connection of the membrane to the midpoint of the deck beam. In such a situation, the tension rays are forced to depart from this point. The resulting arrangement is, as expected, of the type represented in Fig. 12(iv).

5. Rectangular membranes

Completely different wrinkle patterns can be obtained by simply changing the shape of the membrane. While once again neglecting deformation of the pylons, we now consider web bridges supported by rectangular-shaped membranes. The problem reduces to that depicted in Fig. 13. The membrane and beam deck are made of the same elastic, homogeneous and isotropic material ($E = 2.1 \times 10^5$ MPa and $v = 0.1$), as in the foregoing examples.

Fig. 14 schematically again represents the equilibrium state corresponding to $t = 1$ cm and $J_d = 0.01$ m^4 for four different H/L ratio values, i.e., $H/L = 0.25$, 0.5, 1 and 2. The main difference from the cases

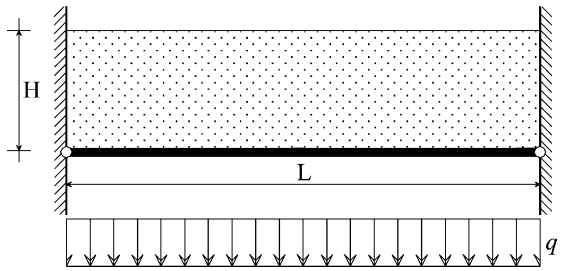

Fig. 13. Web bridge with rectangular-shaped membrane and rigid pylons.

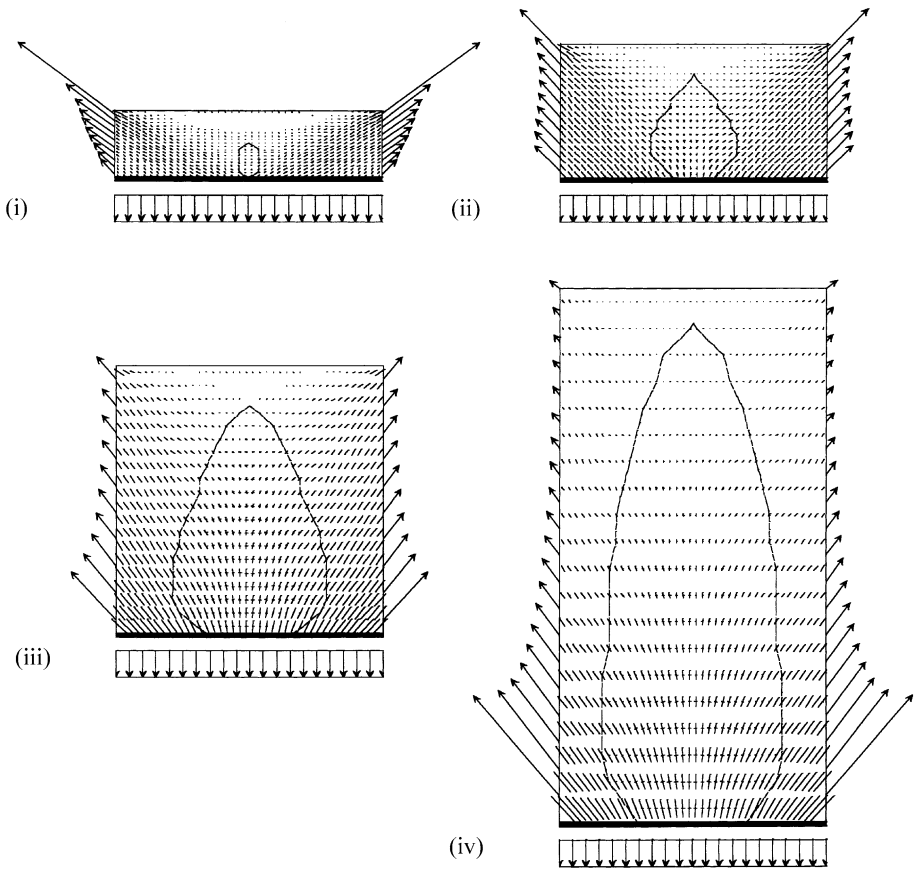

Fig. 14. Influence of the ratio H/L on the stress distribution within the membrane. $L = 100$ m, $J_d = 0.01$ m^4, $t = 1$ cm. (i) $H/L = 0.25$, (ii) $H/L = 0.5$, (iii) $H/L = 1$ and (iv) $H/L = 2$.

considered in Section 4 is that the three different regions, i.e., taut, wrinkled and inactive, now occupy comparable areas. The taut-region contours have been highlighted in the illustrations. Inactive regions are present in correspondence to the upper free edge of the membrane.

Establishing a correspondence between the current stress distribution and possible cable arrangements is more difficult. We place cables along the lines of principal stress in the taut region and maintain the

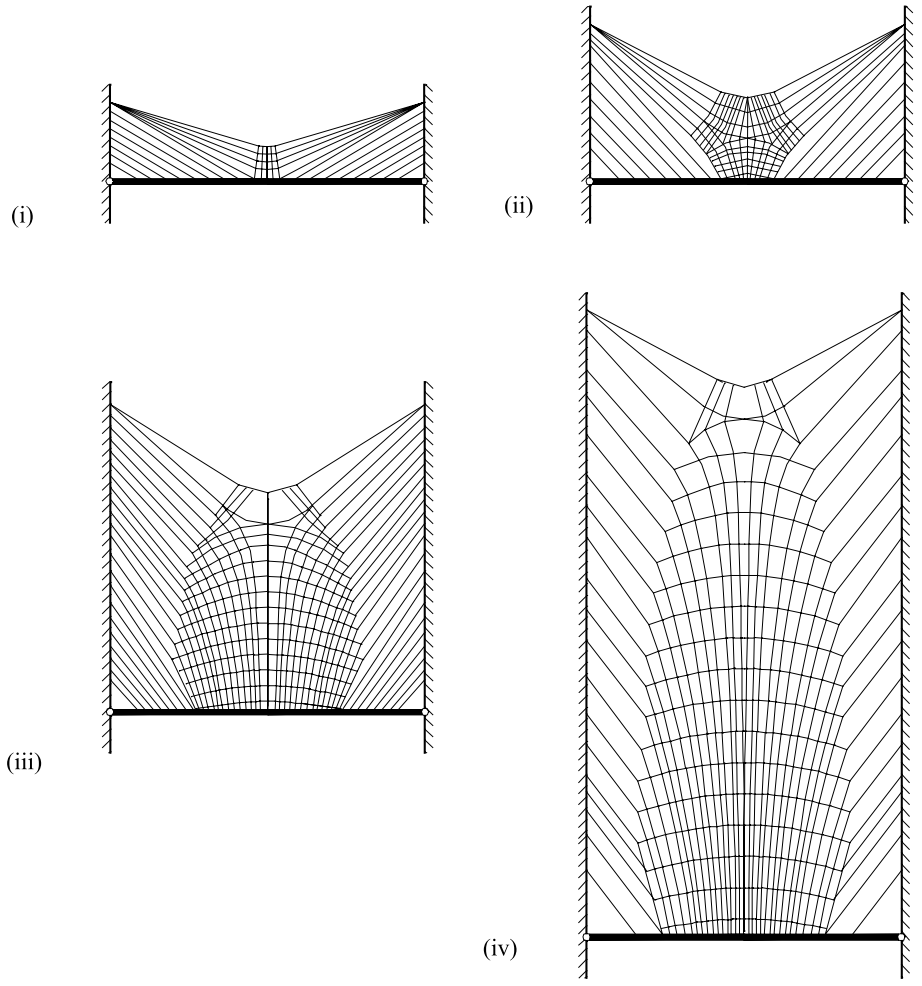

Fig. 15. Cable arrangements for the cases in Fig. 14. $L = 100$ m, $J_d = 0.01$ m^4, $t = 1$ cm. (i) $H/L = 0.25$, (ii) $H/L = 0.5$, (iii) $H/L = 1$ and (iv) $H/L = 2$.

criterion of placing cables along the tension rays in the wrinkled zones. Fig. 15 presents the arrangements resulting for the cases shown in Fig. 14. Now, inclined straight stays sustain the deck in the neighborhood of its extremities, while a cable net upholds the bridge's middle section. This layout recalls some mixed suspended cable-stayed bridges which, according to the systematic studies of Dischinger (1949), were considered to be the most convenient solutions for long-span railroad bridges.

Figs. 16 and 17 again underscore that increasing the membrane's height does not necessarily imply any significant benefit in terms of stiffness. Here, the average stiffness κ and the specific average stiffness κ^*, defined as in Eqs. (4.1) and (4.2), respectively, are reported as a function of H/L. As before, the graph in Fig. 16 tends towards a horizontal asymptote for $H/L \to \infty$. Moreover, Fig. 17 reveals the same optimal value $H/L = 0.5$, corresponding to the case in which the capacity of the membrane is fully exploited.

Naturally, the patterns obtainable when the membrane is partially disconnected from either the beam or pylons are practically innumerable. With the aim of comparing it to Fig. 10, we consider the scheme in Fig. 18. The four cases represented in Fig. 19 show how the tension rays are influenced by the presence of cuts.

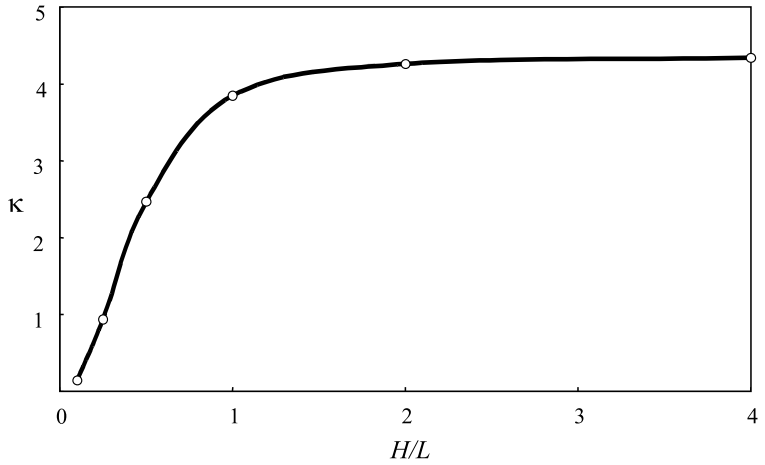

Fig. 16. Overall stiffness of the web bridge as a function of the ratio H/L for varying H and fixed $L = 100$ m, $t = 1$ cm, $J_d = 15.5$ m^4. Loads are considered uniformly distributed on the deck.

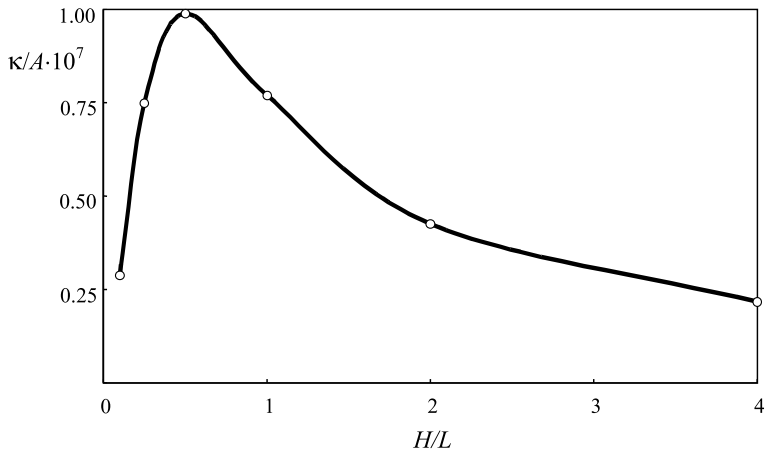

Fig. 17. Specific overall stiffness of the web bridge as a function of the ratio H/L.

As before, the contours of the taut region have been highlighted. For $H_1/H \to 1$, the stayed portion resembles a fan arrangement. An additional cut of length L_1 near the beam's ends produces the formation of triangular inactive regions, equal to those discussed in the corresponding cases in Section 4. However, the presence of the taut zone now yields a hybrid solution, i.e., a mixed suspended and cable-stayed bridge. Such cable arrangements are represented in Fig. 20.

It seems particularly worthwhile to point out the difference between Figs. 12(iv) and 20(iv). Both correspond to $H_1/H = 0.5$ and $L_1/L = 0.5$, but the former refers to a triangular membrane, while in the second the membrane is rectangular. In both cases, the tension rays are forced to originate at the beam midpoint; however, the presence of a taut zone in the rectangular membrane (Fig. 19(iv)) drives the inclined cables to become approximately parallel.

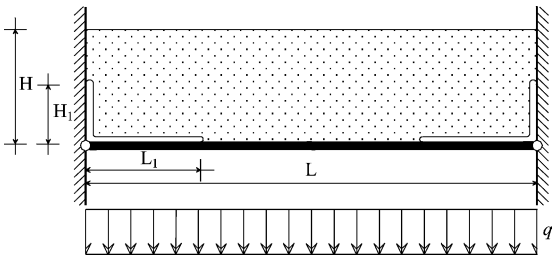

Fig. 18. The case of membranes partially disconnected from pylons and/or deck. Case $H/L = 0.25$, $L = 100$ m, $t = 1$ cm, $J_d = 0.01$ m^4.

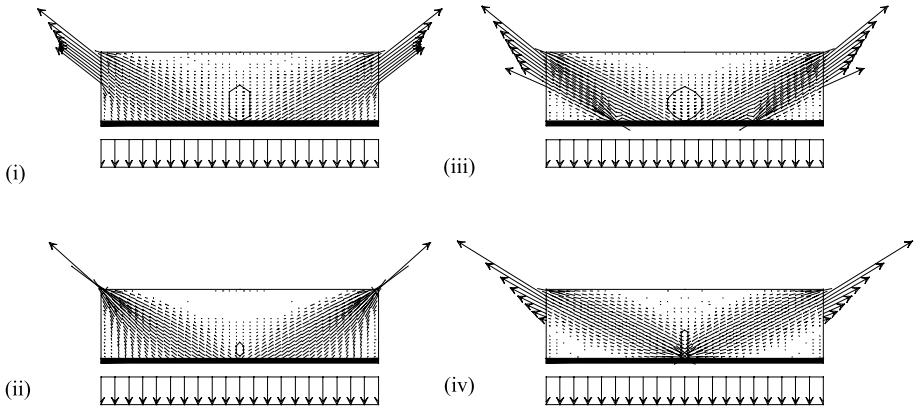

Fig. 19. Equilibrium states of the membrane when partially disconnected near the base of the pylons and along the beam. Case $H/L = 0.25$, $L = 100$ m, $t = 1$ cm, $J_d = 0.01$ m^4. (i) $H_1/H = 0.5$ and $L_1/L = 0$, (ii) $H_1/H = 0.5$ and $L_1/L = 0.25$, (iii) $H_1/H = 1$ and $L_1/L = 0$, (iv) $H_1/H = 0.5$ and $L_1/L = 0.5$.

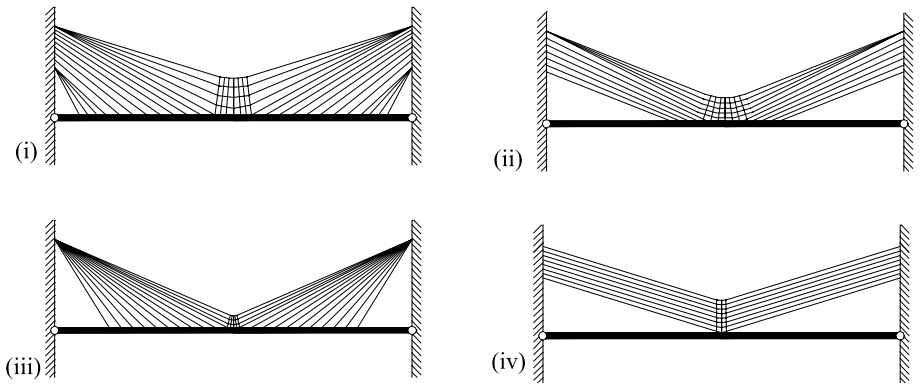

Fig. 20. Cable arrangement resulting from membranes partially disconnected from pylons and deck. Same cases as in Fig. 12.

6. Conclusions

Although the few cases analyzed herein hardly constitute exhaustive treatment, the results obtained provide support for the soundness of the approach. Taking inspiration from the natural wrinkling behavior of membranes to find efficient cable arrangement for tensile structures appears quite promising, and we

believe its full potential remains yet to be realized. The fact that the membrane stress can only be tensile, and that wrinkles, if any, develop "intelligently" according to a "maximum stiffness" criterion, furnish the justification for the proposed procedure that will hopefully prove quite valuable in bridge design.

The main contribution of the present work consists in having identified a theory and developed a finite-element code to describe and calculate the response of elastic membranes under the most varied boundary conditions. The difficult task of identifying the boundary between taut, inactive and wrinkled regions has been overcome through an engineering approach, relying on Pipkin's relaxed energy concept. We have thus been able to analyze relevant cases of bridge design by conceiving of an idealized web bridge, in which the deck is hung on pylons through membranes of different types, essentially triangular or rectangular shaped. The accurate numerical solutions so obtained show good agreement with former approximate ones, confirming that triangular membranes turn out to be nearly entirely wrinkled when loads act on the deck. Moreover, in considering the efficiency of such web bridges, we have arrived at a value of 0.5 for the optimal ratio between pylon height H and total length of the bridge's main span L. In other words, when $H/L = 0.5$, the material making up the membrane is fully exploited, at least with respect to the stiffness of the bridge. In addition, by virtue of the more sophisticated analysis method, we have been able to solve more complex cases. In particular, the analysis of web bridges supported by rectangular shaped membranes reveals the co-existence of all three different possible types of membrane static equilibrium configurations (taut, wrinkled and inactive). As in the triangular membranes, the optimal H/L ratio for rectangular membranes turns out to be 0.5.

Starting with the membrane equilibrium configurations, we have envisaged cable arrangements where rectilinear cables are placed along the direction of the wrinkles, while a cable net, disposed along the lines of principal stress, better interprets the taut regions. An interesting finding is that when triangular-shaped membranes are considered, the resulting cable arrangements are the same as in classical cable-stayed bridges. On the other hand, as rectangular membranes are always taut at the midpoint of the central span (at least for uniformly loaded deck), here the web-bridge solution suggests to use a cable net, where a secondary set of cables is placed at right angle to the principal stays. The resulting cable arrangements show surprising similarities with "hybrid", mixed suspended and cable-stayed solutions, which have been proved to be particularly efficient for long-span bridges subjected to heavy traffic loads. The fact that the shapes obtained via the membrane criterion result similar in type to the classical ones, obtained through long design experience and study, is very encouraging for further studies. As a final point, it may be curious to mention that, based on purely aesthetic considerations, the famous architect Frank Lloyd Wright once designed two bridges sustained by a cable net for the city of Pittsburgh (Riley and Reed, 1994, pp. 284–285). The designs for those bridges (which were never built) show some resemblance to the arrangements discussed in Section 5, where the cable arrangements were based on the web-bridge analysis.

Acknowledgements

G.R. would like to thank Professor T. Galambos for his helpful suggestions during preparation of this work. The skills of Mr. F. Pratelli in preparing the experimental apparatus and Mr. E. Lorenzetti, who had the not easy task of rendering the graphics, are gratefully acknowledged.

References

Barsotti, R., Ligarò, S., 2000. An accurate wrinkled membrane model for analysing the post-critical behaviour of stiffened plate-girders. IASS-IACM 2000, Fourth International Colloquium on Computation of Shell and Spatial Structures, Paper no. 284, Chania-Crete, Greece.

Bhattacharya, K., Dolzmann, G., 2000. Relaxed constitutive relations for phase-transforming materials. J. Mech. Phys. Solids 48, 1493–1517.
Dischinger, F., 1949. Hangebruken fur schwerste Verkehrslasten. Bauingenieur 3–4.
Kang, S., Im, S., 1997. Finite element analysis of wrinkling membranes. ASME J. Appl. Mech. 64, 263–269.
Kondo, K., 1938. The general solution of the flat tension field. J. Soc. Aeron. Sci. Nippon 5, 887–901.
Kondo, K., Iai, T., Moriguti, S., Murasaki, T., 1955. Tension field theory. Memoirs of the Unifying Study of the Basic Problems in Engineering Sciences by means of Geometry, vol. 1, C–V, Gakujutsu Bunken Fukyu-Kai, Tokyo, pp. 61–85.
Jenkins, C.H., Haugen, F., Spicher, W.H., 1998. Experimental measurements of wrinkling in membranes undergoing planar deformation. Exp. Mech. 38, 147–152.
Mansfield, E.H., 1968. Tension field theory. In: Hetenyi, M., Vincenti, W.G. (Eds.), Proceedings of the 12th International Congress on Applied Mechanics, Springer, New York, pp. 305–320.
Mansfield, E.H., 1970. Load transfer via a wrinkled membrane. Proc. Roy. Soc. Lond. A 316, 269–289.
Morrey, C.B., 1952. Quasiconvexity and the lower semicontinuity of multiple integrals. Pacific J. Math. 2, 25–53.
Pipkin, A.C., 1986. The relaxed energy density for isotropic elastic membranes. IMA J. Appl. Math. 36, 85–99.
Reissner, E., 1938. On tension field theory. Proceedings of the Fifth International Congress on Applied Mechanics, pp. 88–92.
Riley, T., Reed, P., 1994. Frank Lloyd Wright Architect. The Museum of Modern Art Edition, New York.
Roddeman, D.G., Drukker, J., Oomens, C.W.J., Janssen, J.D., 1987a. The wrinkling of thin membranes: part I – theory. ASME J. Appl. Mech. 54, 884–887.
Roddeman, D.G., Drukker, J., Oomens, C.W.J., Janssen, J.D., 1987b. The wrinkling of thin membranes: part II – numerical analysis. ASME J. Appl. Mech. 54, 888–892.
Royer-Carfagni, G., 1999. Wrinkled membranes and cable-stayed bridges. ASCE J. Bridge Engng. 4 (1), 56–62.
Steigmann, D.J., 1990. Tension-field theory. Proc. Roy. Soc. Lond. A 429, 141–173.
Steigmann, D.J., Pipkin, A.C., 1989a. Finite deformations of wrinkled membranes. Quart. J. Appl. Math. 42, 427–440.
Steigmann, D.J., Pipkin, A.C., 1989b. Axisymmetric tension fields. J. Appl. Math. Phys. 40, 526–542.
Stein, M., Hedgepeth, J.M., 1961. Analysis of partly wrinkled membranes. NASA Technical Note D-813, Washington, DC.
Timoshenko, S.P., Gere, J.M., 1961. Theory of Elastic Stability, second edition. McGraw-Hill, New York.
Wagner, H., 1929. Ebene Blechwandträger mit sehr dünnem Stegblech. Zeitschr. Flugtechnik u. Motorluftschiffahrt 20, 200–207.
Wu, C.H., 1974. Plane linear wrinkle elasticity without body force. Report Dep. of Materials. Engng., University of Illinois, Chicago Circle.
Wu, C.H., Canfield, T.R., 1981. Wrinkling in finite plane-stress theory. Quart. Appl. Math. 39, 179–199.